Synthesis, Characterization, and Reactivity of an Oxoruthenium(IV) Complex Containing a Bis(oxazoline) Ligand. Crystal Structure of [Ru((*S*)-bpop)(Cl)(trpy)](BF$_4$)

Lisa F. Szczepura, Stephen M. Maricich, Ronald F. See, Melvyn Rowen Churchill, and Kenneth J. Takeuchi*

Department of Chemistry, State University of New York at Buffalo, Buffalo, New York 14260

Received September 30, 1994[⊗]

The synthesis and characterization of two [Ru(L)(O)(trpy)](ClO$_4$)$_2$ complexes (where trpy = 2,2′:6′,2″-terpyridine and L = (*S*)- or (*R*)-bpop = 2,2-bis[2-[4(*S*)- or 4(*R*)-phenyl-1,3-oxazolinyl]]propane) are described. These complexes are among the first high oxidation state oxoruthenium complexes which contain an optically active ligand fixed in a position *cis* to the oxo moiety. The preparations of the precursor materials, [Ru(L)(Cl)(trpy)](BF$_4$) and [Ru(H$_2$O)(L)(trpy)](BF$_4$)$_2$, are also described. A single-crystal X-ray diffraction analysis of [Ru((*S*)-bpop)(Cl)(trpy)](BF$_4$) was undertaken. The crystals belong to the monoclinic system, space group $P2_1$, with a = 12.1507(16) Å, b = 12.3633(10) Å, c = 12.4606 (14) Å, β = 113.332(9)°, V = 1718.9(3) Å^3, and Z = 2. The structure was solved and refined to R = 2.28% and R_w = 2.98% for all 6085 independent reflections. (R = 1.99% for those 5680 reflections with $F_o > 6\sigma(F_o)$.) This is the first report of a (bis(oxazoline))ruthenium single-crystal X-ray structural analysis. To establish the viability of these complexes for ligand effect studies, the pK_a value of the bpop ligand was measured along with the rate constant for the ligand substitution of the aqua ligand of [Ru(H$_2$O)((*R*)-bpop)(trpy)](ClO$_4$)$_2$ by acetonitrile. Our initial substrate oxidation studies of these new (bis(oxazoline))oxoruthenium(IV) complexes with methyl *p*-tolyl sulfide or racemic methyl *p*-tolyl sulfoxide yield results consistent with our previous mechanistic studies on sulfide and sulfoxide oxidations with oxo(phosphine)-ruthenium(IV) complexes.

Introduction

There is a considerable and sustained interest in the quantification of steric and electronic ligand effects on the reactivity of transition metal coordination complexes.[1-4] Parameters used to quantify electronic ligand effects include the following: χ values,[5,6] which are based on the A_1 carbonyl stretching frequency of (PR$_3$)Ni(CO)$_3$ complexes; the NMR chemical shifts (δ) and coupling constants (J) of the ligands;[7] the pK_a values[7a,8] and σ values[9] for the dissociation of the protonated form of the ligand; and the redox potentials of the complexes.[10] Two main parameters used to quantify steric ligand effects are cone angles (θ) defined by Tolman[5] and ligand repulsive energy (E_R[11] and E_R'[1c]) introduced by Brown. The majority of the above ligand studies were limited to monodentate, achiral ligands.

We studied the steric and electronic ligand effects of tertiary phosphine ligands by examining the redox potentials and the kinetics of ligand substitution of the aqua ligand of *cis*-[Ru(H$_2$O)(bpy)$_2$(PR$_3$)](ClO$_4$)$_2$ (bpy = 2,2′-bipyridine and PR$_3$ = tertiary phosphine) complexes.[12] Recently, we extended our ligand effect studies to include bidentate ligands. We investigated the steric and electronic effects of six commonly used bidentate bipyridyl-type ligands by studying the kinetics of ligand substitution of the water ligand of the [Ru(H$_2$O)(L$_2$)(trpy)]$^{2+}$ (trpy = 2,2′:6′,2″-terpyridine and L$_2$ = bidentate bipyridyl-type ligand) complexes by acetonitrile.[13] In addition, by generating the analogous *cis*-[Ru(bpy)$_2$(O)(PR$_3$)](ClO$_4$)$_2$ complexes, we utilized our knowledge of steric and electronic phosphine ligand effects to study the mechanisms involved in the oxidation of alcohols,[14] sulfides, and sulfoxides.[15,16] The above papers illustrate our general strategy of first studying steric and electronic ligand effects via electrochemistry and ligand substitution and then applying the results of the ligand effect studies to redox mechanisms.

Since 1991, there has been a great deal of interest in chiral

[⊗] Abstract published in *Advance ACS Abstracts,* July 1, 1995.

(1) (a) Choi, M.-G.; White, D.; Brown, T. L. *Inorg. Chem.* **1994**, *33*, 5591−5594. (b) Choi, M.-G.; Brown, T. L. *Inorg. Chem.* **1993**, *32*, 1548−1553. (c) Choi, M.-G.; Brown, T. L. *Inorg. Chem.* **1993**, *32*, 5603−5610.
(2) (a) Fernandez, A. L.; Prock, A.; Giering, W. P. *Organometallics* **1994**, *13*, 2767−2772. (b) Wilson, M. R.; Woska, D. C.; Prock, A.; Giering, W. P. *Organometallics* **1993**, *12*, 1742−1752. (c) Wilson, M. S.; Liu, H.; Prock, A.; Giering, W. P *Organometallics* **1993**, *12*, 2044−2050.
(3) (a) Farrar, D. H.; Poe, A. J.; Zheng, Y. *J. Am. Chem. Soc.* **1994**, *116*, 6252−6261. (b) Poe, A. J.; Farrar, D. H.; Zheng, Y. *J. Am. Chem. Soc.* **1992**, *114*, 5146−5152. (c) Chin, M.; Durst, G. L.; Head, S. R.; Bock, P. L.; Mosbo, J. A. *J. Organomet. Chem.* **1994**, *470*, 73−85. (d) Lichtenberger, D. L.; Jatcko, M. E. *J. Coord. Chem.* **1994**, *32*, 79−101.
(4) (a) Davies, M. S.; Aroney, M. J.; Buys, I. E.; Hambley, T. W.; Calvert, J. L. *Inorg. Chem.* **1995**, *34*, 330−336. (b) Aroney, M. J.; Buys, I. E.; Davies, M. S.; Hambley, T. W. *J. Chem. Soc., Dalton Trans.* **1994**, 2827−2834. (c) Dias, P. B.; Depiedade, M. E. M.; Simoes, J. A. M. *Coord. Chem. Rev.* **1994**, *135*, 737−807. (d) Allen, J. V.; Bower, J. F.; Williams, J. M. J. *Tetrahedron: Asymmetry* **1994**, *5*, 1895−1898.
(5) Tolman, C. A. *Chem. Rev.* **1977**, *77*, 313−348.
(6) Bartik, T.; Himmler, T.; Schulte, H.-G.; Seevogel, K. *J. Organomet. Chem.* **1984**, *272*, 29−41.
(7) (a) Allman, T.; Goel, R. G. *Can. J. Chem.* **1982**, *60*, 716−722. (b) Bodner, G. M.; May, M. P.; McKinney, L. E. *Inorg. Chem.* **1980**, *19*, 1951−1958.
(8) Streuli, C. A. *Anal. Chem.* **1960**, *32*, 985−987.
(9) (a) Hansch, C.; Leo, A.; Taft, R. W. *Chem. Rev.* **1991**, *91*, 165−195. (b) Mastryukova, T. A.; Kabachnik, M. I. *Russ. Chem. Rev.* (*Engl. Trans.*) **1969**, *38*, 795−811.
(10) Lever, A. B. P. *Inorg. Chem.* **1990**, *29*, 1271−1285.
(11) Brown, T. L. *Inorg. Chem.* **1992**, *31*, 1286−1294.
(12) Leising, R. A.; Ohman, J. S.; Takeuchi, K. J. *Inorg. Chem.* **1988**, *27*, 3804−3809.
(13) Bessel, C. A.; Margarucci, J. A.; Acquaye, J. H.; Rubino, R. S.; Crandall, J.; Jircitano, A. J.; Takeuchi, K. J. *Inorg. Chem.* **1993**, *32*, 5779−5784.
(14) Muller, J. G.; Acquaye, J. H.; Takeuchi, K. J. *Inorg Chem.* **1992**, *31*, 4552−4557.
(15) Marmion, M. E.; Leising, R. A.; Takeuchi, K. J. *J. Coord. Chem.* **1988**, *19*, 1−16.
(16) Acquaye, J. H.; Muller, J. G.; Takeuchi, K. J. *Inorg. Chem.* **1993**, *32*, 160−165.

0020-1669/95/1334-4198$09.00/0 © 1995 American Chemical Society

bis(oxazoline) ligands.[17-22] These ligands are bidentate nitrogen donor ligands that coordinate in a *cis* fashion to transition metal centers. There are two stereocenters on each bis(oxazoline) ligand, with a C_2 rotation axis relating these two centers. Given the structural similarities between bis(oxazoline) ligands and bipyridyl ligands, we viewed bis(oxazoline) ligands as an opportunity to expand our steric and electronic bidentate ligand effect studies to include an important class of chiral bidentate ligands.

In this paper, we report the synthesis and characterization of the complexes [Ru((*S*)- or (*R*)-bpop)(Cl)(trpy)]$^+$ and [Ru(H_2O)-((*S*)- or (*R*)-bpop)(trpy)]$^{2+}$ ((*S*)- or (*R*)-bpop = 2,2-bis[2-[4(*S*)- or (*R*)-phenyl-1,3-oxazolinyl]]propane). These complexes were fully characterized by means of cyclic voltammetry, UV−visible spectroscopy, ^{1}H NMR spectroscopy, and elemental analysis and represent the first fully characterized (bis(oxazoline))-ruthenium complexes. Onishi and Isagawa reported the syntheses of two bis(oxazoline)ruthenium complexes; however, the complexes were not fully characterized, and reactivity studies were not conducted.[23] In addition, we obtained a single-crystal X-ray structure of [Ru((*S*)-bpop)(Cl)(trpy)](BF_4). This is the first reported crystal structural analysis of a (bis(oxazoline))-ruthenium complex and one of the few reported crystal structure analyses of a bis(oxazoline) ligand bonded to a transition metal center.[18,24,25] Finally, to establish the viability of the aqua(bis-(oxazoline))ruthenium complexes for complete ligand effect studies, the pK_a value of the bpop ligand was measured along with the rate constant for the ligand substitution of the aqua ligand of [Ru(H_2O)((*R*)-bpop)(trpy)](ClO_4)$_2$ by acetonitrile.

We also report in this paper the synthesis and characterization of the first high oxidation state (bis(oxazoline))oxoruthenium(IV) complexes, [Ru(L)(O)(trpy)](ClO_4)$_2$. Notably, the bpop ligand is not oxidized by the oxoruthenium(IV) center, and thus [Ru(L)(O)(trpy)](ClO_4)$_2$ can be isolated and fully characterized. Our initial studies regarding the oxidation of methyl *p*-tolyl sulfide to the corresponding sulfoxide and the oxidation of racemic methyl *p*-tolyl sulfoxide to the corresponding sulfone demonstrate the potential use of (bis(oxazoline))-oxoruthenium complexes as substrate oxidants. These are the first reported oxidations of a sulfide or a sulfoxide by a bis-(oxazoline) transition metal complex.

Experimental Section

Materials. (*S*)-Phenylglycinol was purchased from Aldrich Chemical Co. or Fluka Chemical Co. All reagents were used as received. House distilled water was passed through a Barnstead combination cartridge and an organic removal cartridge before use. All aqueous characterizations and aqueous kinetic measurements were performed using a phosphate buffer (pH = 6.86 KH_2PO_4/Na_2HPO_4, μ = 0.1 M) at 25 ± 1 °C. This pH was chosen because it afforded the maximum stability for both the oxoruthenium(IV) species and the aquaruthenium-(II) species.

Measurements. Electrochemical experiments were carried out in three-electrode, one-compartment cells equipped with a platinum disk (nonaqueous solutions) or glassy carbon (aqueous solutions) working electrode, a platinum wire auxiliary electrode, and a saturated sodium chloride calomel (SSCE) reference electrode. An IBM EC/225 polarographic analyzer equipped with a Houston Instruments Model 100 recorder was used to collect cyclic voltammetric data. Nonaqueous electrochemistry was conducted in methylene chloride using 0.2 M tetra-*n*-butylammonium tetrafluoroborate as the supporting electrolyte while aqueous electrochemistry was conducted using KH_2PO_4/Na_2HPO_4-buffered solution with μ = 0.1 M. ^{1}H NMR spectra were obtained in $CDCl_3$ or CD_3CN, using either a JEOL FX-90Q or a Varian Gemini 300 MHz FT spectrophotometer. Chemical shifts are reported in ppm vs TMS, and resonance splitting patterns are abbreviated by using s for singlet, d for doublet, dd for doublet of doublets, t for triplet, and m for multiplet. Electronic spectra were recorded with a Milton Roy Spectronic 3000 diode array spectrophotometer equipped with a Hewlett Packard 7470A plotter or a Bausch and Lomb Spectronic 2000 spectrophotometer equipped with a Houston Instruments Model 200 recorder. Elemental analyses were performed by Atlantic Microlabs (Norcross, GA). Infrared spectroscopic measurements used Nujol mulls on KBr plates, and a Nicolet FT-IR spectrophotometer. Gas chromatographic experiments utilized a Shimadzu GC-8A gas chromatograph equipped with a megabore column (J&W Scientific, i.d. = 0.53 mm, length = 30 m) containing a DB-5 stationary phase. HPLC experiments utilized a Shimadzu LC-6A pump equipped with a Chiracel OB column (Diacel, 4.6 mm × 250 mm) using a 15:85 isopropyl alcohol/*n*-hexane mobile phase with a variable-wavelength detector set at 248 nm.

pK_a Determination. The pK_a value of the protonated form of the bpop ligand was determined using the method of Streuli,[8] which was developed for the titration of organic bases and water-insoluble phosphines. The bpop dissolved in nitromethane (2.2×10^{-5} M) was titrated against a solution of $HClO_4$ in nitromethane. The titration curve was plotted as potential (mV) vs quantity of titrant (mL) in order to determine the HNP (half-neutralization point). The HNP value of 2,2′-bipyridine was determined as a standard, and the aqueous pK_a value for the protonated form of bpop was calculated using the equation $\Delta HNP = -63.80(pK_a) + 261.8$ (where ΔHNP = HNP(bpop) − HNP-(bpy)). This equation describes the relationship between the pK_a(H_2O) and ΔHNP (nitromethane) for a series of pyridine-type nitrogen donor ligands.[13] The calculated pK_a for the protonated form of bpop is 3.21 ± 0.07 (average of five runs).

Product Distributions and Kinetic Measurements. The oxidation studies of methyl *p*-tolyl sulfide and racemic methyl *p*-tolyl sulfoxide were conducted in acetonitrile under a dinitrogen atmosphere. The oxoruthenium(IV) concentration was 4.5×10^{-3} M while the substrate concentrations were 1.0×10^{-2} M, and the reaction time for both oxidations was 3 h. The reaction products were quantitatively determined by means of gas chromatography where all of the sulfur-containing materials were recovered within 10% of the starting sulfur amounts. The percent enantiomeric excess (%ee = |%*R* − %*S*|) of the product mixture was determined by HPLC analysis.

The rate constant of acetonitrile ligand substitution of the aqua ligand of [Ru(H_2O)((*R*)-bpop)(trpy)]$^{2+}$ was measured spectrophotometrically (Milton Roy Spectronic 401 spectrophotometer) in pH = 6.86 buffer at 25 °C, using modifications of the techniques and procedures reported previously.[12] In a typical experiment, 1 mL of one of eight solutions of varying concentration of acetonitrile (0.54−5.4 M) was added to 2 mL of a 2.4×10^{-4} M [Ru(H_2O)((*R*)-bpop)(trpy)]$^{2+}$ solution. The solutions were mixed using a disposable pipet, and the absorbance versus time plots were recorded.

Preparation of Compounds. (*S*)- or (*R*)-bpop. This procedure is a modified version of that reported by Corey.[26] A 1.22 g sample of (*S*)- or (*R*)-phenylglycinol (8.9 mmol) was combined with 1.24 mL of Et_3N (8.9 mmol) in CH_2Cl_2 at 0 °C. Next, 0.748 g of dimethylmalonyl chloride[27] (4.4 mmol) was added, and the solution was stirred overnight at room temperature. The following day, 1.40 mL of $SOCl_2$ (distilled over $P(OC_6H_5)_3$) (19.2 mmol) was added, and the solution was heated

(17) Brookhart, M.; Wagner, M. I.; Balavoine, G. G. A.; Haddou, H. A. *J. Am. Chem. Soc.* **1994**, *116*, 3641−3642.
(18) Pfaltz, A. *Acc. Chem. Res.* **1993**, *26*, 339−345.
(19) Koskinen, A. M. P.; Hassila, H. *J. Org. Chem.* **1993**, *58*, 4479−4480.
(20) Evans, D. A.; Faul, M. M.; Bilodeau, M. T.; Anderson, B. A.; Barnes, D. M. *J. Am. Chem. Soc.* **1993**, *115*, 5328−5329.
(21) Corey, E. J.; Wang, Z. *Tetrahedron Lett.* **1993**, *34*, 4001−4004.
(22) Ohkita, K.; Kurosawa, H.; Hasegawa, T.; Hirao, T.; Ikeda, I. *Organometallics* **1993**, *12*, 3211−3215.
(23) Onishi, M.; Isagawa, K. *Inorg. Chim. Acta* **1991**, *179*, 155−156.
(24) Bolm, C.; Wieghardt, K.; Zehnder, M.; Ranff, T. *Chem. Ber.* **1991**, *124*, 1173−1180.
(25) Evans, D. A.; Woerpel, K. A.; Scott, M. J. *Angew. Chem., Intl. Ed. Engl.* **1992**, *31*, 430−432.
(26) Corey, E. J.; Imai, N.; Zhang, H.-Y. *J. Am. Chem. Soc.* **1991**, *113*, 728−729.
(27) Pierce, C. C.; Elliel, E. L.; Convery, R. J. *J. Org. Chem.* **1957**, *22*, 347−348.

at reflux for 2 h. The crude product ((*S*)- or (*R*)-dpm-Cl) was isolated from hexanes and purified using column chromatography (silica gel with 5:95 MeOH/CH_2Cl_2). A 0.722 g sample of white powder was obtained (40% yield); mp = 174−176 °C. To generate the (*S*)- or (*R*)-bpop ligand, 10 mL of 0.54 M NaOH was added to 0.385 g of pure (*S*)- or (*R*)-dpm-Cl in 400 mL of 50:50 MeOH/H_2O and the mixture was heated at reflux for 1 h. After cooling to room temperature, the solution was extracted with 3 × 50 mL of toluene. The toluene layers were combined and dried with sodium sulfate. Removal of the solvent with a rotary evaporator resulted in a cloudy, colorless oil which was pure by ^1H and ^{13}C NMR analyses.

[Ru((*S*)- or (*R*)-bpop)(Cl)(trpy)](BF$_4$). A 0.424 g sample of $RuCl_3$(trpy)[28] (0.96 mmol) and 0.322 g of (*S*)- or (*R*)-bpop (0.96 mmol) were combined with 0.22 mL of Et_3N (1.6 mmol) and 0.058 g of LiCl (1.36 mmol) in 88 mL of 75:25 ethanol/H_2O. The solution was heated at reflux for 4 h and then filtered hot through a medium frit. The addition of a filtered solution of $NaBF_4$ (2.7 g in 4 mL H_2O) to the filtrate and subsequent rotary evaporation induced precipitation of the crude material (0.836 g). The solid was purified by column chromatography on alumina with 5:95 MeOH/CH_2Cl_2 as the eluent and then recrystallized several times from CH_2Cl_2/toluene. After drying in vacuo overnight, 0.225 g (30% yield) of dark purple crystals was obtained. ^1H NMR ($CDCl_3$, 400 MHz): δ 1.94 (s, 3H), 1.99 (s, 3H), 3.76 (dd, 2H), 4.15 (t, 1H), 5.18 (m, 2H), 5.90 (d, 2H), 6.50−8.50 (20 H). ^{13}C NMR ($CDCl_3$, 300 MHz): δ 25.69, 27.86, 40.15, 69.81, 70.35, 75.22, 75.91, 121.10, 121.64, 123.05, 123.20, 124.17, 126.83, 127.23, 128.14, 128.63, 129.03, 129.12, 129.31, 132.52, 135.93, 136.66, 138.27, 141.25, 150.99, 153.46, 158.98, 159.45, 159.64, 160.20, 169.65, 171.46. $E_{1/2}$(CH_2Cl_2) = 0.78 V vs SSCE. UV−vis (CH_2Cl_2) λ, nm (ϵ, L mol^{-1} cm^{-1}): 679 (1200), 620 (1900), 519 (5000), 372 (sh), 325 (29 000), 277 (19 000). Anal. Calcd for $C_{36}H_{33}N_5O_2RuClBF_4$: C, 54.66; H, 4.20. Found: C, 54.56; H, 4.24.

[Ru(H$_2$O)((*S*)- or (*R*)-bpop)(trpy)](BF$_4$)$_2$·2H$_2$O. A 0.201 g sample of [Ru(L)(Cl)(trpy)](BF_4) (0.25 mmol) was combined with 0.077 g of $AgBF_4$ (0.40 mmol) in 40 mL of 75:25 acetone/H_2O, and the mixture was heated at reflux under dinitrogen for 1 h. After cooling to room temperature, the solution was passed through a fine frit to remove the AgCl produced during the reaction; then the volume of the filtrate was reduced with a rotary evaporator. Chilling of the remaining solution in an ice bath caused the [Ru(H_2O)(L)(trpy)](BF_4)$_2$ to precipitate. The reddish brown solid was isolated and washed dropwise with cold H_2O, yielding 0.168 g (77% yield) of product. $E_{1/2}$(CH_2Cl_2) = 1.05 V vs SSCE. UV−vis (CH_2Cl_2) λ, nm (ϵ, L mol^{-1} cm^{-1}): 620 (sh), 555 (sh), 487 (4300), 360 (sh), 320 (32 000), 276 (20 000). UV−vis (pH = 6.86 KH_2PO_4/Na_2HPO_4, μ = 0.1 M) λ, nm (ϵ, L mol^{-1} cm^{-1}): 635 (sh), 570 (sh), 497 (4200), 360 (sh), 320 (32 000), 276 (20 000). Anal. Calcd for $C_{36}H_{35}N_5O_3B_2F_8Ru$·2$H_2O$: C, 48.24; H, 4.39. Found: C, 48.21; H, 4.35.

Caution! While we have used perchlorate as a counterion with a number of ruthenium complexes without incident, perchlorate salts of metal complexes with organic ligands are potentially explosive. Care should be exercised in using a spatula or stirring rod to mechanically agitate any solid perchlorate. These complexes, as well as other perchlorate salts, should be handled only in small quantities.[29]

[Ru(CH$_3$CN)((*R*)-bpop)(trpy)](ClO$_4$)$_2$·0.40Et$_2$O. A 0.100 g sample of [Ru(H_2O)((*R*)-bpop)(trpy)](ClO_4)$_2$ was stirred overnight under a blanket of dinitrogen in 13 mL of acetonitrile. The following day, the volume of the acetonitrile was reduced with a rotary evaporator, and the remaining solution was eluted through an alumina column. The red-orange band was collected and reduced to dryness under vacuum. The remaining solid was dissolved in a small amount of acetonitrile and added to stirring Et_2O. The solid that precipitated was collected and placed in a vacuum oven (39 °C) overnight. A 0.063 g sample of red-orange solid was obtained (53% yield). ^1H NMR (CD_3CN, 300 MHz): δ 1.82 (s, 3H), 1.94 (s, 3H), 2.02 (s, 3H), 3.82 (m, 1H), 4.00 (m, 1H), 4.17 (t, 1H), 4.92 (m, 1H), 5.30 (t, 1H), 5.80 (m, 1H), 6.00 (d, 2H), 6.70−8.50 (19H). $E_{1/2}$(CH_3CN) = 1.17 V vs SSCE; $E_{1/2}$(CH_2Cl_2) = 1.26 V vs SSCE. UV−vis (CH_3CN) λ, nm (ϵ, L mol^{-1} cm^{-1}): 585 (sh), 525 (sh), 446 (4300), 313 (33 000), 272 (21 000). Anal. Calcd for $C_{38}H_{36}N_6O_{10}Cl_2Ru$·0.40$Et_2O$: C, 49.76; H, 4.41. Found: C, 49.50; H, 4.13.

Table 1. Crystallographic Data for [Ru((*S*)-bpop)(Cl)(trpy)](BF_4)

chem formula	$C_{36}H_{33}BClF_4N_5O_2Ru$	fw	791.0
crystal system	monoclinic	space group	$P2_1$ (No. 4)
a	12.1507(16) Å	T	22 ± 1 °C
b	12.3633(10) Å	λ	0.710 73 Å
c	12.4606(14) Å	ϱ_{calcd}	1.528 g/cm^3
β	113.332(9)°	μ	5.85 cm^{-1}
V	1718.9(3) Å^3	$R(F)^a$	2.28%
Z	2	$R_w(F)^b$	2.98%

^{a} $R(F) = [\sum||F_o| - |F_c||/\sum|F_o|] \times 100$ (%). ^{b} $R_w(F) = [\sum w(|F_o| - |F_c|)^2/\sum w|F_o|^2]^{1/2} \times 100$ (%).

[Ru((*S*)- or (*R*)-bpop)(O)(trpy)](ClO$_4$)$_2$·1.5H$_2$O. A 0.76 mL portion of Ce(IV) (0.5 N in 6 N $HClO_4$) was added dropwise to 0.022 g of [Ru(H_2O)(L)(trpy)](BF_4)$_2$ dissolved in 40 mL of H_2O, which caused an immediate color change of the solution from clear red-brown to orange, in addition to producing a precipitate. The mixture was stirred for 2 min, chilled for 2 min, and filtered. The solid was washed with cold H_2O and stored in a freezer until further use. A 0.012 g sample of a golden yellow solid, characterized as [Ru(L)(O)(trpy)](ClO_4)$_2$·1.5H_2O, was obtained (54% yield). $E_{1/2}$(pH = 6.86 KH_2PO_4/Na_2HPO_4, μ = 0.1 M) = 0.41 V vs SSCE. UV−vis (pH = 6.9 KH_2PO_4/Na_2HPO_4, μ = 0.1 M) λ, nm (ϵ, L mol^{-1} cm^{-1}): 333 (sh), 322 (12 000), 277 (15 000). UV−vis (CH_2Cl_2) λ, nm (ϵ, L mol^{-1} cm^{-1}): 336 (sh), 322 (15 000), 278 (17 000). IR (Nujol mull): 792 cm^{-1} sh ($\nu_{Ru=O}$). Anal. Calcd for $C_{36}H_{33}N_5O_{11}Cl_2Ru$·1.5$H_2O$: C, 47.48; H, 3.98. Found: C, 47.51; H, 3.87.

[Ru((*S*)-bpop)(^{18}O)(trpy)](ClO$_4$)$_2$. A 0.025 g sample of [Ru(H_2O)((*S*)-bpop)(trpy)]$^{2+}$ was slurried in 2.0 mL of $H_2{}^{18}O$ (90%; 90.97 atom % ^{18}O; 3.49 atom % ^{16}O and 0.014 atom % D), purchased from Alfa Products (Morton Thiokol, Inc.), for 4 h. The $H_2{}^{18}O$ was then removed under reduced pressure, and the resulting solid was dissolved in 45 mL of $H_2{}^{16}O$. Next, 0.89 mL of Ce(IV) solution (0.5 N in 6 N $HClO_4$) was quickly added. The solution was stirred for 1 min, chilled for 1 min, and then rapidly filtered, and the solid was washed with chilled $H_2{}^{16}O$.

Collection of X-ray Diffraction Data for [Ru((*S*)-bpop)(Cl)(trpy)](BF$_4$). A dark-red single crystal (0.30 × 0.35 × 0.40 mm), sealed into a thin-walled capillary, was mounted and aligned on a Siemens R3m/V four-circle diffractometer. Determination of Laue symmetry, unit cell parameters, and orientation matrix were carried out as described previously.[30] Intensity data (Mo Kα, λ = 0.710 73 Å) were collected at 22 ± 1 °C using graphite-monochromatized radiation. A complete sphere of data was collected for the range 2θ = 5.0−50.0°, with index ranges of $-14 \le h \le 14$, $-14 \le k \le 14$, $-14 \le l \le 14$. The minimum and maximum transmission coefficients were 0.8303 and 0.9240, respectively. Details of the structure are provided in Table 1. The systematic absences $0k0$ for $k = 2n + 1$ are consistent with the noncentrosymmetric space group $P2_1$ (No. 4) or the centrosymmetric space group $P2_1/m$ (No. 11). The former is the more probable with Z = 2 and with a chiral ligand and was later confirmed by the successful solution of the structure. Data were corrected for Lorentz and polarization effects and for absorption. The 12 169 reflections were merged to a (point-group) unique set of 6085 reflections with the excellent internal consistency of R(int) = 0.82%. The number of reflections greater than 6σ were 5680.

Solution and Refinement of the Crystal Structure of [Ru((*S*)-bpop)(Cl)(trpy)](BF$_4$). All calculations were performed on a VAX station 3100 computer with use of the Siemens SHELXTL PLUS program package.[31] The analytical scattering factors for neutral atoms were used and corrected for the real ($\Delta f'$) and imaginary ($\Delta f''$)

(28) Leising, R. A.; Kubow, S. A.; Churchill, M. R.; Buttrey, L. A.; Ziller, J. W.; Takeuchi, K. J. *Inorg. Chem.* **1990**, *29*, 1306−1312.
(29) Wosley, W. C. *J. Chem. Educ.* **1973**, *50*, A335−A337.
(30) Churchill, M. R.; Lashewycz, R. A.; Rotella, F. J. *Inorg. Chem.* **1977**, *16*, 265.
(31) SHELXTL PLUS; Siemens Analytical Instrument Corp.: Madison, WI, 1988.

components of anomalous dispersion.[32] The structure was solved by direct methods and difference-Fourier syntheses. All non-hydrogen atoms were located, and their positional and thermal parameters were refined. (The origin of the polar space group $P2_1$ was fixed by assigning the value $y = 0$ for the y coordinate of the ruthenium atom.) Hydrogen atoms were included in calculated positions with $d(C-H) = 0.96$ Å.[33] The parameter η, refined as a multiplier to the $\Delta f''$ values, was used to ascertain the absolute configuration of the crystal and its constituent molecules; the final value of $\eta = 1.06(3)$ shows that the correct enantiomer has been defined. The structure refined smoothly to convergence ($(\Delta/\sigma)_{max} = 0.001$) with $R = 2.28\%$ and $R_w = 2.98\%$ for all 6085 point-group-independent reflections and $R = 1.99\%$ and $R_w = 2.63\%$ for those 5680 reflections with $F_o > 6\sigma(F_o)$. A final difference-Fourier map was "clean" with features only in the range $-0.56 \rightarrow +0.74$ e/Å^3. Final atomic coordinates are collected in Table 2.

Results

Syntheses. The procedure used to bind bpop to ruthenium was modeled after the procedure used to coordinate bidentate bipyridyl-type ligands to $[Ru(Cl)_3(trpy)]$.[13] The $[Ru(H_2O)(L)(trpy)]^{2+}$ complexes were synthesized by reacting the corresponding chlororuthenium(II) complex with Ag^+ in the presence of water.[34,35] Ce(IV) was used as an oxidant to convert $[Ru(H_2O)(L)(trpy)]^{2+}$ to $[Ru(L)(O)(trpy)]^{2+}$.[34,35]

The solid $[Ru(L)(O)(trpy)]^{2+}$ complexes are stable for 1−2 days when stored in a freezer. The aquaruthenium complexes were also stored in a freezer while the chlororuthenium complexes were stored under ambient conditions, and both of these could be stored indefinitely. The analytical data for all newly synthesized complexes are described below. Elemental analyses are reported in the Experimental Section and indicate analytically pure materials, where some of the solids contain solvent molecules of crystallization or waters of hydration.

NMR Spectroscopy. The ^1H and ^{13}C NMR spectra of $[Ru((S)\text{-bpop})(Cl)(trpy)](BF_4)$ (Figure 1) show evidence of both bpop and trpy coordination, where the (*S*)-bpop ligand loses C_2 symmetry upon coordination. A comparison of the ^1H NMR spectrum of the free ligand with that of $[Ru((S)\text{-bpop})(Cl)(trpy)](BF_4)$ shows that the singlet resonance ($\delta = 1.64$ ppm, 6H) assigned to the methyl groups of the propane chain in the free ligand splits into two resonances ($\delta = 1.94$ and 1.99 ppm) upon coordination. The three resonances at $\delta = 3.76$, 5.18, and 5.90 ppm in the ^1H NMR spectrum of $[Ru((S)\text{-bpop})(Cl)(trpy)](BF_4)$, integrating for two protons each, were assigned to the protons on the oxazoline ring. In addition, the complex series of resonances ranging from $\delta = 6.50$ to 8.50 ppm (20H) were assigned to the aromatic protons of the phenyl substituents on the bpop ligand and to the terpyridine protons.

Interestingly, a triplet integrating for one proton was observed at $\delta = 4.15$ ppm. After examining the crystal structure of $[Ru((S)\text{-bpop})(Cl)(trpy)](BF_4)$, we assigned this triplet to a phenyl proton from the bpop ligand that is directed into a pyridine ring of the trpy ligand (see crystal structure section below). The ring current effect resulting from a phenyl proton of bpop being directed into the center of an aromatic pyridine ring of trpy explains the observed upfield shift of approximately 3 ppm compared to the chemical shift of this proton in the uncoordinated ligand.[36]

Infrared Spectroscopy. A new peak was observed at 792 cm^{-1} in the IR spectrum of the $[Ru((S)\text{-bpop})(O)(trpy)](ClO_4)_2$ complex compared to that of the corresponding aquaruthenium(II) complex. A number of oxoruthenium(IV) complexes are

Table 2. Atomic Coordinates ($\times 10^4$) and Equivalent Isotropic Displacement Coefficients (Å$^2 \times 10^3$)

	x	*y*	*z*	*U*(eq)[a]
Ru(1)	1457(1)	0	1770(1)	28(1)
Cl(1)	204(1)	461(1)	−226(1)	42(1)
N(11)	2549(2)	1342(2)	1896(2)	41(1)
C(12)	2089(3)	2279(2)	2134(3)	45(1)
C(13)	2641(4)	3268(3)	2173(4)	69(2)
C(14)	3684(4)	3306(3)	1978(4)	80(2)
C(15)	4166(4)	2362(3)	1782(4)	76(2)
C(16)	3569(3)	1397(3)	1737(3)	55(1)
N(21)	604(2)	1111(2)	2241(2)	33(1)
C(22)	997(3)	2146(2)	2354(2)	39(1)
C(23)	383(3)	2943(2)	2676(3)	49(1)
C(24)	−624(3)	2667(2)	2868(2)	47(1)
C(25)	−1026(3)	1610(2)	2725(2)	41(1)
C(26)	−402(2)	844(2)	2380(2)	34(1)
N(31)	2(2)	−883(2)	1726(2)	31(1)
C(32)	−754(2)	−298(2)	2080(2)	33(1)
C(33)	−1818(2)	−729(2)	2048(3)	44(1)
C(34)	−2147(3)	−1758(3)	1630(3)	49(1)
C(35)	−1418(3)	−2332(2)	1225(3)	47(1)
C(36)	−357(2)	−1870(2)	1293(2)	38(1)
N(41)	2305(2)	−1293(2)	1271(2)	32(1)
C(42)	2829(2)	−2112(2)	1878(2)	36(1)
O(43)	3075(2)	−2950(2)	1309(2)	49(1)
C(44)	2424(3)	−2729(2)	80(3)	49(1)
C(45)	2157(2)	−1510(2)	33(2)	38(1)
N(51)	2595(2)	−443(2)	3471(2)	32(1)
C(52)	3203(2)	−1305(2)	3825(2)	35(1)
O(53)	3922(2)	−1366(2)	4961(2)	50(1)
C(54)	3932(3)	−312(3)	5440(2)	54(1)
C(55)	2891(2)	288(2)	4496(2)	41(1)
C(61)	2990(2)	−820(2)	−316(2)	39(1)
C(62)	2528(2)	−138(3)	−1275(2)	43(1)
C(63)	3284(3)	469(3)	−1631(3)	53(1)
C(64)	4512(3)	426(3)	−1013(3)	63(1)
C(65)	4976(3)	−245(3)	−66(3)	68(2)
C(66)	4223(3)	−875(3)	287(3)	56(1)
C(71)	1847(3)	466(2)	4857(2)	42(1)
C(72)	1073(3)	−357(2)	4820(2)	46(1)
C(73)	143(3)	−198(3)	5188(3)	63(2)
C(74)	19(4)	796(4)	5620(3)	76(2)
C(75)	807(4)	1623(4)	5686(3)	79(2)
C(76)	1709(3)	1483(3)	5289(3)	57(1)
C(1)	3204(3)	−2317(2)	3165(2)	41(1)
C(2)	4469(3)	−2819(3)	3657(3)	67(1)
C(3)	2301(4)	−3114(3)	3328(3)	65(2)
B(1C)	6438(4)	−196(5)	3966(4)	78(2)
F(1C)	5384(3)	56(5)	3985(4)	178(3)
F(2C)	6937(3)	679(3)	3683(4)	135(2)
F(3C)	6323(5)	−998(4)	3211(5)	201(4)
F(4C)	7130(4)	−525(4)	5008(4)	198(3)

[a] Equivalent isotropic *U* defined as one-third of the trace of the orthogonalized U_{ij} tensor.

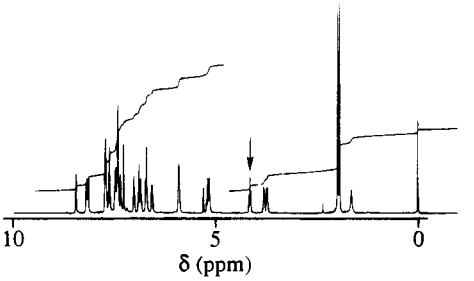

Figure 1. ^1H NMR spectrum of $[Ru((S)\text{-bpop})(Cl)(trpy)](BF_4)$ in $CDCl_3$. The arrow points to the resonance which is shifted upfield due to a ring current effect. Resonances at $\delta = 5.30$ (methylene chloride), 2.36 (toluene) are solvents used in the purification of this material, and water ($\delta = 1.65$) is also present.

(32) *International Tables for X-Ray Crystallography*; Kynoch Press: Birmingham, England, 1974; Vol. 4, pp 99−101, 149−150.
(33) Churchill, M. R. *Inorg. Chem.* **1973**, *12*, 1213.
(34) Marmion, M. E.; Takeuchi, K. J. *J. Am. Chem. Soc.* **1988**, *110*, 1472−1480.
(35) Kubow, S. A.; Marmion, M. E.; Takeuchi, K. J. *Inorg. Chem.* **1988**, *27*, 2761−2767.

reported to have Ru(IV)=O stretches in the 773−845 cm^{-1} region;[37] therefore, we believe that the stretch observed at 792 cm^{-1} in the IR spectrum of [Ru((*S*)-bpop)(O)(trpy)]$(ClO_4)_2$ is due to the Ru(IV)=O stretch. To confirm our assignment, we performed an ^{18}O-labeling experiment. The IR spectrum of [Ru((*S*)-bpop)(^{18}O)(trpy)]$^{2+}$ showed only a small shoulder at 792 cm^{-1} while a new peak appeared at 757 cm^{-1}. The decrease (35 cm^{-1}) in wavenumber upon ^{18}O labeling is consistent with a Hooke's law approximation for the Ru(IV)=O stretch.

Electrochemistry. The cyclic voltammogram of [Ru((*S*)-bpop)(Cl)(trpy)]$^+$ displays one couple with $E_{1/2}$ = 0.78 V, a peak current ratio ($i_{p,c}/i_{p,a} \approx 1.0$), and a linear ($r^2 = 0.998$) plot of the anodic peak current ($i_{p,a}$) versus the square root of the scan rate ($\nu^{1/2}$).[38] The separation between the cathodic and anodic peak potentials (110 mV) was the same as the peak potential separation for the known reversible ferrocene/ferrocenium couple (internal standard).[39]

The cyclic voltammogram of [Ru(H_2O)((*S*)−bpop)(trpy)]$^{2+}$ in methylene chloride displays one couple at 1.05 V ($i_{p,c}/i_{p,a} \approx 1.0$, ΔE_p = 100 mV), 270 mV higher than the $E_{1/2}$ of the corresponding chlororuthenium complex recorded under the same conditions. This increase in the potential of the Ru(III/II) couple upon substitution of a chloride ligand for a water ligand is typical of other chloro- to aquaruthenium conversions.[34,35] The cyclic voltammogram of the [Ru(H_2O)-((*S*)-bpop)(trpy)]$^{2+}$ complex recorded in a solution buffered at pH = 6.86 displays two reversible couples, one at 0.41 V and another (much smaller compared to the first) at 0.54 V. On the basis of our previous experience with analogous aquaruthenium(II) complexes,[34,35] we assigned the wave at 0.41 V to the Ru(III)−OH/Ru(II)−H_2O couple and the wave at 0.54 V to the Ru(IV)=O/Ru(III)−OH couple.

Aquaruthenium(II) complexes typically undergo ligand substitution of the aqua ligand by acetonitrile.[12,13,34] We observed this reactivity with the [Ru(H_2O)((*S*)-bpop)(trpy)]$^{2+}$ complex. Acetonitrile was added to the electrochemical cell containing [Ru(H_2O)((*S*)-bpop)(trpy)]$^{2+}$ in methylene chloride, and the voltammograms were obtained as a function of time. The couple at 1.03 V was observed to decrease in size while a new couple grew in at 1.24 V. After approximately 30 min, only the wave at 1.24 V was observed, indicating a quantitative conversion of the aquaruthenium complex to the [Ru(CH_3CN)-((*S*)-bpop)(trpy)]$^{2+}$ complex.

Electronic Spectroscopy. The UV−vis spectra of the [Ru-((*S*)- or (*R*)-bpop)(Cl)(trpy)]$^+$ complexes display six absorption bands. Four of these bands (λ_{max} = 679, 620, 519, 372 nm) have extinction coefficients in the range 1000−5000 L mol^{-1} cm^{-1}. These values are consistent with metal-to-ligand dπ (Ru) → π^* (trpy or bpop) charge transfer (MLCT) transitions.[34,35] The two high-energy transitions (λ_{max} = 325, 277 nm) have extinction coefficients of 29 000 and 19 000 L mol^{-1} cm^{-1}, respectively. These transitions are consistent with π (trpy or bpop) → π^* (trpy or bpop) ligand-localized transitions which are also characteristic of related complexes.[34,35]

The UV−vis spectra of the [Ru(H_2O)(L)(trpy)]$^{2+}$ complexes also display six absorption bands: four MLCT transitions and two ligand-localized transitions. The MLCT bands of the aquaruthenium complexes appear to shift to shorter wavelengths ($\Delta\lambda$ = 32−65 nm) compared to those of the chlororuthenium complexes. These shifts are believed to be caused by the increase in the formal charge of the ruthenium center of the aquaruthenium complex compared to the chlororuthenium complex, which stabilizes the ruthenium dπ orbitals relative to the π^* orbitals (trpy or bpop), causing the MLCT transitions to be shifted to shorter wavelengths.[34] The ligand-localized transitions shift only slightly ($\Delta\lambda$ = 1−5 nm) when the chloride ligand is replaced by a water ligand.

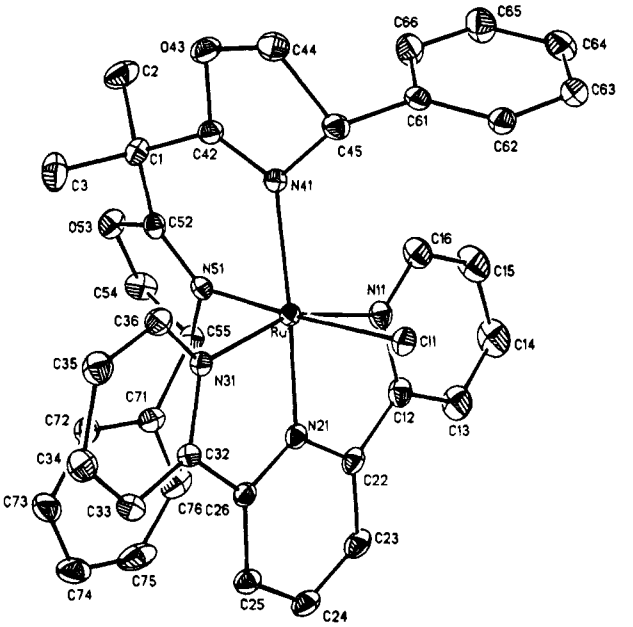

Figure 2. Geometry of the [Ru((*S*)-bpop)(Cl)(trpy)]$^+$ cation showing the atomic labeling scheme. This is an ORTEP2 diagram with 30% probability contours for the vibration ellipsoids of non-hydrogen atoms. All hydrogen atoms are omitted for clarity.

When acetonitrile is added to an aqueous solution of [Ru-(H_2O)((*S*)-bpop)(trpy)]$^{2+}$, the substitution of the water ligand by acetonitrile can be observed spectrophotometrically. The final spectrum was found to match that of the independently prepared [Ru(CH_3CN)((*S*)-bpop)(trpy)]$^{2+}$ complex. Notably, the MLCT bands of the [Ru(CH_3CN)((*S*)-bpop)(trpy)]$^{2+}$ complex occur at higher energies than those of [Ru(H_2O)((*S*)-bpop)-(trpy)]$^{2+}$, as is observed for analogous complexes undergoing similar ligand substitution reactions.[12]

Oxoruthenium(IV) complexes typically do not display intense absorption bands in the visible region.[34,35] The [Ru(L)(O)-(trpy)]$^{2+}$ complexes displayed only a small shoulder at 400 nm along with three intense bands in the UV region at 277, 322, and 333 nm. Since the UV−vis spectra of the [Ru(L)(O)-(trpy)]$^{2+}$ complexes are significantly different from the spectra of the [Ru(H_2O)(L)(trpy)]$^{2+}$ and [Ru(CH_3CN)(L)(trpy)]$^{2+}$ complexes, the redox reaction producing either one of these ruthenium(II) complexes can be easily monitored using spectroscopic techniques.

Crystal Structure of [Ru((*S*)-bpop)(Cl)(trpy)](BF$_4$). There are only two previous X-ray crystallographic studies of monomeric transition metal complexes containing neutral bis-(oxazoline) ligands reported in the literature.[18,24] Since these two studies involve four-coordinate complexes, specifically tetrahedral zinc(II) and square planar palladium(II) centers, our study is notable because it is the first X-ray crystal structure analysis involving a neutral bis(oxazoline) ligand bonded to a six-coordinate ruthenium(II) center. The [Ru((*S*)-bpop)(Cl)-(trpy)]$^+$ cation is illustrated in Figure 2. Interatomic distances

(36) Becker, E. D. *High Resolution NMR Theory and Chemical Applications*, 2nd ed.; Academic Press: New York, 1980; p 97.
(37) Che, C.-M.; Yam, V. W.-W. *Adv. Inorg. Chem.* **1993**, *39*, 233−325.
(38) Kissinger, P. T.; Heineman, W. R. *Laboratory Techniques in Electroanalytical Chemistry*; Marcel Dekker, Inc.: New York, 1984; p 82.
(39) Gagne, R. R.; Koval, C. A.; Lisensky, G. C. *Inorg. Chem.* **1980**, *19*, 2854−2855.

Table 3. Bond Lengths (Å)

Ru(1)−Cl(1)	2.414(1)	Ru(1)−N(11)	2.091(3)
Ru(1)−N(21)	1.946(3)	Ru(1)−N(31)	2.060(2)
Ru(1)−N(41)	2.124(2)	Ru(1)−N(51)	2.094(2)
N(11)−C(12)	1.369(4)	N(11)−C(16)	1.333(5)
C(12)−C(13)	1.386(5)	C(12)−C(22)	1.466(5)
C(13)−C(14)	1.383(7)	C(14)−C(15)	1.370(6)
C(15)−C(16)	1.386(6)	N(21)−C(22)	1.354(3)
N(21)−C(26)	1.342(4)	C(22)−C(23)	1.388(5)
C(23)−C(24)	1.379(5)	C(24)−C(25)	1.382(4)
C(25)−C(26)	1.383(4)	C(26)−C(32)	1.481(4)
N(31)−C(32)	1.372(4)	N(31)−C(36)	1.336(3)
C(32)−C(33)	1.385(4)	C(33)−C(34)	1.374(4)
C(34)−C(35)	1.376(5)	C(35)−C(36)	1.381(4)
N(41)−C(42)	1.274(3)	N(41)−C(45)	1.504(4)
C(42)−O(43)	1.354(4)	C(42)−C(1)	1.505(4)
O(43)−C(44)	1.444(3)	C(44)−C(45)	1.537(4)
C(45)−C(61)	1.513(4)	N(51)−C(52)	1.273(3)
N(51)−C(55)	1.487(3)	C(52)−O(53)	1.339(3)
C(52)−C(1)	1.497(4)	O(53)−C(54)	1.432(4)
C(54)−C(55)	1.535(3)	C(55)−C(71)	1.521(5)
C(61)−C(62)	1.387(4)	C(61)−C(66)	1.387(4)
C(62)−C(63)	1.388(5)	C(63)−C(64)	1.382(5)
C(64)−C(65)	1.369(5)	C(65)−C(66)	1.398(6)
C(71)−C(72)	1.373(4)	C(71)−C(76)	1.404(5)
C(72)−C(73)	1.392(5)	C(73)−C(74)	1.374(7)
C(74)−C(75)	1.381(7)	C(75)−C(76)	1.380(7)
C(1)−C(2)	1.541(5)	C(1)−C(3)	1.547(5)
B(1C)−F(1C)	1.327(7)	B(1C)−F(2C)	1.353(7)
B(1C)−F(3C)	1.336(8)	B(1C)−F(4C)	1.303(6)

and angles are collected in Tables 3 and 4. The crystal consists of an array of [Ru((*S*)-bpop)(Cl)(trpy)]$^+$ cations and [BF_4]$^-$ anions in a 1:1 stoichiometry. The ruthenium(II) cation has a distorted octahedral environment with a *mer*-trpy ligand (Ru(1)−N(11) = 2.091(3) Å, Ru(1)−N(21) = 1.946(3) Å, Ru(1)−N(31) = 2.060(2) Å), a *cis*-(*S*)-bpop ligand (Ru(1)−N(41) = 2.124(2) Å, Ru(1)−N(51) = 2.094(2) Å), and a chloride ligand (Ru(1)−Cl(1) = 2.414(1) Å).

A comparison of the bond lengths and bond angles of free trpy (2,2′:6′,2″-terpyridine) to those of trpy in [Ru((*S*)-bpop)(Cl)(trpy)]$^+$ shows the greatest distortions occur around the 2- and 6-positions of the central pyridine ring. These observations are similar to previous observations made regarding coordinated and free trpy.[40] The (*S*)-bpop ligand is coordinated to ruthenium with Ru−N bond lengths of Ru(1)−N(41) = 2.124(2) Å and Ru(1)−N(51) = 2.094(2) Å (average = 2.109 Å). Literature values for Ru−N bond lengths range from 2.01 to 2.20 Å for a variety of imine and pyridine-like ligands;[41−43] thus our average distance of 2.109 Å is reasonable for the (*S*)-bpop ligand. The Ru−Cl bond length measured at 2.414(1) Å is a typical Ru−Cl bond length.[43−45] The N(41)−Ru−N(51) bond angle of 84.1(1)° is distorted from ideal octahedral geometry, but it is consistent with the data reported by Pfaltz for allyl(bis(oxazoline))palladium complexes which contain N−Pd−N angles of 88 and 84°.[18]

The oxazoline rings appear to be relatively planar, with the deviations from the mean plane being 0.08 and 0.05 Å for the oxazoline rings containing N(41) and N(51), respectively. The dihedral angle between the two oxazoline rings defined by N(41)−C(42)−C(45) and N(51)−C(52)−C(55) is 22.3°.

Table 4. Bond Angles (deg)

Cl(1)−Ru(1)−N(11)	90.7(1)	Cl(1)−Ru(1)−N(21)	87.1(1)
N(11)−Ru(1)−N(21)	79.4(1)	Cl(1)−Ru(1)−N(31)	85.0(1)
N(11)−Ru(1)−N(31)	159.2(1)	N(21)−Ru(1)−N(31)	80.1(1)
Cl(1)−Ru(1)−N(41)	93.3(1)	N(11)−Ru(1)−N(41)	104.6(1)
N(21)−Ru(1)−N(41)	176.0(1)	N(31)−Ru(1)−N(41)	96.0(1)
Cl(1)−Ru(1)−N(51)	177.3(1)	N(11)−Ru(1)−N(51)	89.2(1)
N(21)−Ru(1)−N(51)	95.5(1)	N(31)−Ru(1)−N(51)	96.0(1)
N(41)−Ru(1)−N(51)	84.1(1)	Ru(1)−N(11)−C(12)	112.8(2)
Ru(1)−N(11)−C(16)	129.0(2)	C(12)−N(11)−C(16)	118.2(3)
N(11)−C(12)−C(13)	121.4(4)	N(11)−C(12)−C(22)	115.0(3)
C(13)−C(12)−C(22)	123.6(3)	C(12)−C(13)−C(14)	119.2(4)
C(13)−C(14)−C(15)	119.3(4)	C(14)−C(15)−C(16)	119.1(4)
N(11)−C(16)−C(15)	122.7(4)	Ru(1)−N(21)−C(22)	119.3(2)
Ru(1)−N(21)−C(26)	119.2(2)	C(22)−N(21)−C(26)	121.4(3)
C(12)−C(22)−N(21)	113.3(3)	C(12)−C(22)−C(23)	127.2(3)
N(21)−C(22)−C(23)	119.5(3)	C(22)−C(23)−C(24)	119.4(3)
C(23)−C(24)−C(25)	120.3(3)	C(24)−C(25)−C(26)	118.5(3)
N(21)−C(26)−C(25)	120.8(2)	N(21)−C(26)−C(32)	112.8(2)
C(25)−C(26)−C(32)	126.3(3)	Ru(1)−N(31)−C(32)	112.9(2)
Ru(1)−N(31)−C(36)	129.4(2)	C(32)−N(31)−C(36)	117.3(2)
C(26)−C(32)−N(31)	114.9(2)	C(26)−C(32)−C(33)	123.1(3)
N(31)−C(32)−C(33)	121.7(2)	C(32)−C(33)−C(34)	119.6(3)
C(33)−C(34)−C(35)	118.9(3)	C(34)−C(35)−C(36)	119.0(3)
N(31)−C(36)−C(35)	123.4(3)	Ru(1)−N(41)−C(42)	127.6(2)
Ru(1)−N(41)−C(45)	124.0(1)	C(42)−N(41)−C(45)	107.2(2)
N(41)−C(42)−O(43)	117.3(2)	N(41)−C(42)−C(1)	129.5(3)
O(43)−C(42)−C(1)	113.2(2)	C(42)−O(43)−C(44)	105.6(2)
O(43)−C(44)−C(45)	104.2(2)	N(41)−C(45)−C(44)	101.4(2)
N(41)−C(45)−C(61)	111.8(2)	C(44)−C(45)−C(61)	114.1(3)
Ru(1)−N(51)−C(52)	129.0(2)	Ru(1)−N(51)−C(55)	123.3(2)
C(52)−N(51)−C(55)	107.6(2)	N(51)−C(52)−O(53)	117.3(2)
N(51)−C(52)−C(1)	129.5(2)	O(53)−C(52)−C(1)	113.1(2)
C(52)−O(53)−C(54)	106.5(2)	O(53)−C(54)−C(55)	104.6(2)
N(51)−C(55)−C(54)	102.1(2)	N(51)−C(55)−C(71)	113.3(2)
C(54)−C(55)−C(71)	112.0(2)	C(45)−C(61)−C(62)	120.2(2)
C(45)−C(61)−C(66)	121.2(2)	C(62)−C(61)−C(66)	118.5(3)
C(61)−C(62)−C(63)	120.8(2)	C(62)−C(63)−C(64)	120.4(3)
C(63)−C(64)−C(65)	119.2(4)	C(64)−C(65)−C(66)	120.8(3)
C(61)−C(66)−C(65)	120.2(3)	C(55)−C(71)−C(72)	121.5(3)
C(55)−C(71)−C(76)	118.9(3)	C(72)−C(71)−C(76)	119.5(3)
C(71)−C(72)−C(73)	121.3(3)	C(72)−C(73)−C(74)	119.0(4)
C(73)−C(74)−C(75)	120.3(5)	C(74)−C(75)−C(76)	121.1(4)
C(71)−C(76)−C(75)	118.8(3)	C(42)−C(1)−C(52)	112.3(2)
C(42)−C(1)−C(2)	109.0(3)	C(52)−C(1)−C(2)	109.6(2)
C(42)−C(1)−C(3)	108.4(2)	C(52)−C(1)−C(3)	107.8(3)
C(2)−C(1)−C(3)	109.8(3)	F(1C)−B(1C)−F(2C)	110.6(5)
F(1C)−B(1C)−F(3C)	110.8(5)	F(2C)−B(1C)−F(3C)	110.1(5)
F(1C)−B(1C)−F(4C)	107.6(5)	F(2C)−B(1C)−F(4C)	109.3(4)
F(3C)−B(1C)−F(4C)	108.4(5)		

The chirality of the bpop ligand was determined crystallographically by η refinement and is the same as the chirality of the amino acid that was used in the synthesis of this material. This is important to note because it proves that the reaction conditions used to coordinate the bpop ligand to the ruthenium center did not induce racemization. As mentioned above in the NMR spectroscopy section, it appears that either H(72A) or H(76A) (protons on the phenyl substituent of the (*S*)-bpop ligand) is the proton that is shifted upfield by approximately 3 ppm in the ^{1}H NMR spectrum of [Ru((*S*)-bpop)(Cl)(trpy)]$^+$ due to a ring current effect of the trpy ligand.

Reactivity. In addition to the electrochemical experiment described above (see electrochemistry section), the aqua ligand substitution of [Ru(H_2O)(L)(trpy)]$^{2+}$ by acetonitrile was monitored spectroscopically, and the reaction displayed isosbestic behavior for more than 3 half-lives. Kinetic studies of this reaction were monitored at the λ_{max} of the most intense MLCT band of the initial aquaruthenium(II) complex. Plots of $\ln[(A_0 - A_\infty)/(A - A_\infty)]$ vs t gave linear fits with the slope being equal to k_{obs}. The value of k was obtained by plotting k_{obs} versus the acetonitrile concentration for the eight different solutions (see the supplementary Table S1 for a list of the kinetic data). The

(40) Bessel, C. A.; See, R. F.; Jameson, D. L.; Churchill, M. R.; Takeuchi, K. J. *J. Chem. Soc., Dalton Trans.* **1992**, 3223−3228.
(41) Rillema, D. P.; Jones, D. S.; Woods, C.; Levy, H. A. *Inorg. Chem.* **1992**, *31*, 2935−2938.
(42) Coe, B. J.; Meyer, T. J.; White, P. S. *Inorg. Chem.* **1993**, *32*, 4012−4020.
(43) Szczepura, L. F.; Muller, J. G.; Bessel, C. A.; See, R. F.; Janik, T. S.; Churchill, M. R.; Takeuchi, K. J. *Inorg. Chem.* **1992**, *31*, 859−869.
(44) Das, B. K.; Chakravarty, A. R. *Inorg. Chem.* **1992**, *31*, 1395−1400.
(45) Claire, K. S.; Hill, A. F. *Inorg. Chem.* **1992**, *31*, 2906−2908.

value of k for $[Ru(H_2O)((R)\text{-bpop})(trpy)]^{2+}$ was determined to be 1.6×10^{-4} ($\pm 1.4 \times 10^{-5}$) M^{-1} s^{-1}.

The mechanism of acetonitrile substitution reactions for ruthenium(II) complexes is known to proceed via a dissociative interchange (I_D).[12] The mechanism is shown schematically in eqs 1 and 2, with the associated rate law shown in eq 3, where

$$(L)(trpy)Ru{-}OH_2^{2+} + CH_3CN \overset{K_0}{\rightleftharpoons} [(L)(trpy)Ru{-}OH_2\text{- - -}CH_3CN]^{2+} \quad (1)$$

$$[(L)(trpy)Ru{-}OH_2\text{- - -}CH_3CN]^{2+} \xrightarrow{k_0} (L)(trpy)Ru{-}NCCH_3^{2+} + H_2O \quad (2)$$

$$\text{rate} = \frac{K_0 k_0 [Ru(OH_2)(L)(trpy)^{2+}][CH_3CN]}{1 + K_0[CH_3CN]} \quad (3)$$

K_0 represents a preequilibrium that exists prior to ligand exchange (L = (*S*)- or (*R*)-bpop). However, a purely second-order rate equation will hold when $K_0[CH_3CN]$ is much less than 1, which allows eq 3 to simplify to eq 4;[46] (where $k = k_0K_0$). This is what is observed for our kinetic system, where (4) represents the rate law for our reactions.

$$\text{rate} = k[Ru(OH_2)(L)(trpy)^{2+}][CH_3CN] \quad (4)$$

The oxidation of methyl *p*-tolyl sulfide by $[Ru((S)\text{-bpop})(O)(trpy)]^{2+}$ was also monitored spectrophotometrically. In this reaction (shown schematically in eqs 5 and 6, where SRR′ = methyl *p*-tolyl sulfide and OSRR′ = methyl *p*-tolyl sulfoxide), an intermediate (λ_{max} = 500 nm) is observed and is then further

$$(L)(trpy)Ru{=}O^{2+} + SRR' \rightarrow (L)(trpy)Ru{-}O{-}SRR'^{2+} \quad (5)$$

$$(L)(trpy)Ru{-}O{-}SRR'^{2+} + CH_3CN \rightarrow (L)(trpy)Ru{-}NCCH_3^{2+}\ OSRR' \quad (6)$$

reacted, producing the $[Ru(CH_3CN)((S)\text{-bpop})(trpy)]^{2+}$ complex (λ_{max} = 445 nm) as the final product. The initial reaction has one isosbestic point at 429 nm while the second reaction has two isosbestic points at 400 and 472 nm. The intermediate at λ_{max} = 500 nm is proposed to be the O-bound sulfoxide complex, where Meyer observed similar spectral changes in the oxidation of dimethyl sulfide by $[Ru(trpy)(bpy)(O)]^{2+}$.[47] However, it is interesting to note that we did not observe any intermediates in the oxidation of dibutyl and *para*-substituted methyl phenyl sulfides by *cis*-$[Ru(bpy)_2(O)(PR_3)]^{2+}$ complexes in acetonitrile.[15,16] The rapid dissociation of the O-bound sulfoxide intermediate for the oxo(phosphine)ruthenium complexes was attributed to the steric bulk of the phosphine ligand positioned *cis* to the oxo moiety. The oxidation of (*R*)- or (*S*)-methyl *p*-tolyl sulfoxide by $[Ru((S)\text{-bpop})(O)(trpy)]^{2+}$ displayed isosbestic behavior in acetonitrile without formation of a detectable intermediate (as shown schematically by eq 7, where O_2SRR' = methyl *p*-tolyl sulfone).[15,16,47]

$[Ru((S)\text{-bpop})(O)(trpy)](ClO_4)_2$ oxidizes methyl *p*-tolyl sulfide to the corresponding sulfoxide without production of sulfone (63.8 ± 8.1% yield, 11.8 ± 2.0% ee (*R*)) and, in a separate reaction, oxidizes racemic methyl *p*-tolyl sulfoxide to the corresponding sulfone (66.8 ± 6.0% yield, 27.0 ± 0.8% ee (*R*)). Similarly, $[Ru((R)\text{-bpop})(O)(trpy)](ClO_4)_2$ oxidizes methyl *p*-tolyl sulfide to the corresponding sulfoxide without production of sulfone (69.3 ± 5.4% yield, 11.4 ± 1.8% ee (*S*)) and, in a separate reaction, oxidizes racemic methyl *p*-tolyl sulfoxide to the corresponding sulfone (72.4 ± 8.4% yield, 23.8 ± 2.1% ee (*S*)).

$$(L)(trpy)Ru{=}O^{2+} + OSRR' \rightarrow (L)(trpy)Ru{-}NCCH_3^{2+} + O_2SRR' \quad (7)$$

Discussion

The oxidations of methyl *p*-tolyl sulfide and racemic methyl *p*-tolyl sulfoxide by $[Ru((S)\text{-bpop})(O)(trpy)](ClO_4)_2$ produce an enantiomeric excess of the (*R*) sulfoxide. For the oxidation of racemic methyl *p*-tolyl sulfoxide by $[Ru((S)\text{-bpop})(O)(trpy)](ClO_4)_2$, oxidation of (*S*)-methyl *p*-tolyl sulfoxide is favored; however, from the product distribution of the oxidation of the prochiral sulfide, it appears that oxidation at the pro-*re* face (pro-*R*)[48] of methyl *p*-tolyl sulfide is favored. Other researchers have observed this inversion of chiral selectivity primarily in biological systems,[49] but to the best of our knowledge, only one group of researchers, Montanari et al., has proposed an explanation for this type of stereoselectivity.[50] If we apply Montanari's interpretation of stereoselectivity to our ruthenium complexes, we can rationalize that $[Ru((S)\text{-bpop})(O)(trpy)](ClO_4)_2$ should preferentially produce the (*R*) sulfoxide in the oxidation of the sulfide while, in the oxidation of racemic sulfoxide, (*S*)-methyl *p*-tolyl sulfoxide should react faster, producing sulfone and sulfoxide with the (*R*) enantiomer formed in excess.

The % ee value obtained from the oxidation of methyl *p*-tolyl sulfide is approximately half of the %ee value obtained from the oxidation of racemic methyl *p*-tolyl sulfoxide by $[Ru(L)(O)(trpy)](ClO_4)_2$. Recently, we reported the mechanisms of oxidation of *para*-substituted methyl phenyl sulfides and *para*-substituted methyl phenyl sulfoxides by a family of achiral oxoruthenium complexes, *cis*-$[Ru(bpy)_2(O)(PR_3)](ClO_4)_2$ (bpy = 2,2′-bipyridine; $PR_3 = P(p\text{-}C_6H_4X)_3$, X = OMe, Me, H, F, CF_3); sulfide oxidation was found to occur by means of a single electron transfer (SET) mechanism while sulfoxide oxidation was found to occur by means of an S_N2 mechanism where the sulfur atom nucleophilically attacks the oxoruthenium moiety.[16] If we assume that the oxidation of methyl *p*-tolyl sulfoxide by $[Ru(L)(O)(trpy)](ClO_4)_2$ involves a similar S_N2 mechanism and that the oxidation of methyl *p*-tolyl sulfide by $[Ru(L)(O)(trpy)](ClO_4)_2$ involves an SET mechanism, then we can rationalize our %ee value differences. Since an S_N2 mechanism requires a closer and more directed approach of the target substrate to the oxoruthenium(IV) center than an SET mechanism, it is expected that the chiral ligand of $[Ru(L)(O)(trpy)](ClO_4)_2$ has a greater effect on the %ee values of the sulfoxide in the oxidation of methyl *p*-tolyl sulfoxide to the corresponding sulfone than in the oxidation of methyl *p*-tolyl sulfide to the corresponding sulfoxide.

Conclusions

We reported the synthesis and full characterization of several ruthenium complexes which use a chiral bis(oxazoline) ligand,

(46) Wilkins, R. G. *The Study of Kinetics and Mechanism of Reactions of Transition Metal Complexes*; Allyn and Bacon, Inc.: Boston, 1974; p 187.
(47) Roecker, L.; Dobson, J. C.; Vining, W. J.; Meyer, T. J. *Inorg. Chem.* **1987**, *26*, 779.
(48) Groves, J. T.; Viski, P. *J. Org. Chem.* **1990**, *55*, 3628−3634.
(49) (a) Sugimoto, T.; Kokubo, T.; Miyazaki, J.; Tanimoto, S. *Bioorg. Chem.* **1981**, *10*, 311−323. (b) Holland, H. L.; Rand, C. G.; Viski, P.; Brown, F. M. *Can. J. Chem.* **1991**, *69*, 1989−1993.
(50) (a) Folli, U.; Iarossi, D.; Montanari, F.; Torre, G. *J. Chem. Soc. C* **1968**, 1317−1322. (b) Folli, U.; Iarossi, D.; Montanari, F. *J. Chem. Soc. C* **1968**, 1372−1374.

and part of our characterization included the single-crystal X-ray structural analysis of [Ru((*S*)-bpop)(Cl)(trpy)](BF_4). The rate constant of ligand substitution of the aqua ligand of [Ru(H_2O)-((*R*)-bpop)(trpy)](ClO_4)$_2$ by acetonitrile and the pK_a value of the bis(oxazoline) ligand were both readily measurable; thus two important quantifiable reaction properties are available for future bis(oxazoline) ligand effect studies. Further, the bis-(oxazoline) ligands are quite suitable for ligand effect studies because the bis(oxazoline) substituents can be varied from methyl to phenyl to isopropyl to *tert*-butyl by changing the amino alcohols used to synthesize the ligands.

Among the complexes prepared here were the first oxo-ruthenium(IV) complexes containing a chiral C_2 symmetric (bis-(oxazoline)) ligand *cis* to the oxo moiety. These [Ru(L)(O)-(trpy)]$^{2+}$ complexes proved to be active oxidants of organic substrates such as sulfides and sulfoxides. The outcome of our substrate oxidation studies was rationalized in terms of (1) our previous mechanistic studies conducted on the oxidation of alkyl aryl sulfides and sulfoxides by oxo(phosphine)ruthenium(IV) complexes and (2) a scheme devised by Montanari used to predict the configuration of the enantiomer formed in excess for sulfide and sulfoxide oxidations.

Acknowledgment. We thank the National Science Foundation for partial financial support of this work (Grant No. CHE 9120602), the ARCO Chemical Co., and Johnson Matthey Aesar/Alfa for their generous loan of $RuCl_3 \cdot 3H_2O$. Purchase of the Siemens R3m/V diffractometer was made possible by Grant 89-13733 from the Chemical Instrumentation Program of the National Science Foundation. We also acknowledge Professor J. Keister for the use of his Nicolet FT-IR spectrophotometer.

Supporting Information Available: Listings of the kinetic data (Table S1), anisotropic thermal parameters (Table S2), and calculated positions for hydrogen atoms (Table S3) (4 pages). For ordering information, see any current masthead page.

IC941108G